Nucleus accumbens neuron subtype translatome signatures in socially stressed females

Gautam Kumar[1], Daniela Franco[1], Mahashweta Basu[2], Jimmy Olusakin[1], Rianne Campbell[1], Seth A. Ament[2,3,4], Megan E. Fox[5], Mary Kay Lobo[1,4]*

1. University of Maryland School of Medicine, Department of Neurobiology
2. Institute for Genome Sciences, University of Maryland School of Medicine
3. Maryland Psychiatric Research Center, Department of Psychiatry, University of Maryland School of Medicine
4. UM-MIND Institute for Neuroscience Discovery, University of Maryland School of Medicine
5. Penn State College of Medicine, Department of Anesthesiology & Perioperative Medicine

*Correspondence should be addressed to: mklobo@som.umaryland.edu

Abstract

Major depressive disorder (MDD) disproportionately affects women, yet the molecular mechanisms underlying female vulnerability remain poorly understood. The nucleus accumbens (NAc), a reward circuitry hub, is central to stress- and depression-related pathology. While NAc medium spiny neuron (MSN) transcriptional adaptations have been characterized in stressed male rodents, much less is known about female adaptations. To address this, we exposed female D1-Cre-RiboTag and A2A-Cre-RiboTag mice to chronic witness defeat stress (CWDS) and classified them as high- or low-social interactors. Ribosome-associated mRNA was isolated from MSN subtypes and analyzed by RNA sequencing, differential gene expression analysis (DEG), and weighted gene co-expression network analysis (WGCNA). Cross-species consensus WGCNA with male mouse and human transcriptomic datasets was performed to identify conserved, sex-specific signatures. We detected 9 differentially expressed genes (DEGs) in D1-MSNs and 630 in A2A-MSNs (FDR < 0.05). In D1-MSNs, DEGs were primarily upregulated in low interactors and enriched for energy homeostasis and cell adhesion. A2A-MSN DEGs included upregulated structural genes and downregulated neurotransmission-related genes. WGCNA identified 9 significant D1- and 5 significant A2A-MSN modules, with the most impacted enriched for PI3K-Akt-mTOR signaling and regulated by Nf1. Consensus analysis revealed a stress-associated, sex- and subtype-specific module enriched for PI3K-Akt-mTOR signaling conserved across mice and humans. These findings reveal female-specific MSN transcriptional adaptations to chronic social stress and implicate PI3K-Akt-mTOR signaling as a convergent molecular pathway. By highlighting MSN subtype-specific vulnerabilities, this work suggests potential therapeutic targets for alleviating stress-induced pathology in women with MDD.

Introduction

Major depressive disorder, (MDD), is expected to become the foremost cause of disease burden worldwide by 2030 [1]. Treatment has limited success, with 30% of patients resistant or relapsing [2]. To uncover the mechanisms underlying vulnerability to MDD, researchers use chronic stress paradigms to model disrupted affective behaviors. Chronic social stress paradigms have face validity and better mirror the psychosocial nature of human stress [3-9]. These paradigms, however, are often limited to male-only use[10]. Given sex differences in MDD symptomatology, antidepressant response, and increased incidence in women, female subjects are crucial for understanding MDD neuropathology [10]. Social stress models employing female subjects have emerged in recent years [8, 12, 14]. One social stress paradigm, chronic witness defeat stress (CWDS) adapts chronic social defeat stress (CSDS) by exposing mice to witnessed - rather than physical - defeat allowing modeling of affective dysfunction in females [8, 11]. Unlike other alternative models, employing female aggressors, male odorants or chemogenic manipulation, CWDS models the psychological aspects of social trauma, making it more translatable, as sources of human stress tend to be interpersonal/emotional [12-14].

Understanding mechanisms in brain regions mediating depression symptoms is essential for novel therapies. One such region is the nucleus accumbens (NAc), a key integration center in the motivational circuitry [7, 15, 16]. MDD patients show reduced NAc volume and blunted activation, while deep brain stimulation of the NAc alleviates symptoms in resistant cases, driving interest in NAc-targeted treatments [17]. Medium spiny neurons (MSNs) make up over 90% of NAc neurons and include D1- and D2-type subtypes distinguished by dopamine receptor expression and other GPCRs like adenosine 2a receptor (A2A) [18, 19]. Activation of D1-MSNs promotes reward behavior, while inhibition increases vulnerability to anhedonia [20, 21]. Increased D1-MSN intrinsic excitability with reduced synaptic input, and enhanced D2/A2A-MSN synaptic input, associate with social avoidance and stress susceptibility [20]. However, how sex differences in these subtypes contribute to MDD remains unclear.

Using female CWDS and celltype-specific RNA-seq via D1-Cre-RiboTag and A2A-Cre-RiboTag mice, we profiled NAc MSN subtype-specific translatomes. We identified differentially expressed genes and co-expression networks in D1- and A2A-MSNs of low and high SI females. We then used publicly available transcriptomics data to identify consensus networks in male and female mice and human MDD patients, identifying unique sex-specific molecular signatures relevant to MDD [22, 23]. Given the chronic, relapsing course of MDD,

101 this study may reveal molecular targets for MDD and other stress-related psychiatric
102 disorders.
103

104 ***Materials and Methods***

105 **Animals**

106 Experiments followed Institutional Animal Care and Use Committee guidelines at University
107 of Maryland School of Medicine (UMSOM). Mice were given ad libitum food/water and
108 housed in a 12:12 h light:dark cycle in the UMSOM vivarium. Homozygous Rpl22HA
109 ("RiboTag", RT) mice crossed with D1-Cre (line FK150)/A2A-Cre (line KG 139) mice generated
110 female D1-Cre-RT & A2A-Cre-RT mice used for subtype-specific RNA-seq [24]. All transgenic
111 mice were on a C57Bl/6 background and 8-10 weeks old at the start. Male CD-1 retired
112 breeders (>4 months, Charles River) served as CWDS aggressors; male C57BL6
113 conspecifics were intruders.

114 **Chronic Witness Defeat Stress (CWDS)**

115 CWDS was performed as described [14]. Female experimental mice, housed behind a
116 plexiglass divider in a cage, witnessed a male CD-1 defeat a male intruder for 10 min. This
117 occurred between 9:00-14:00 ZT each day. After each witness episode the witness mouse
118 was then housed opposite a novel CD-1 for 24-hour sensory interaction. This repeated for 10
119 days with a novel CD-1 resident each day. Control mice were pair-housed with sex-matched
120 conspecifics, separated by a divider, for 10 days. After the last witness episode mice were
121 singly housed through the three-chamber social interaction on day 11 followed by tissue
122 collection on day 12.

123 **Three-chamber Social Interaction Test**

124 24 hours post-defeat, mice underwent 3 chamber social interaction (3ChSI) testing between
125 9:00-14:00 ZT. Mice started in the center of a three-chambered arena (60 × 40 cm), with
126 empty cups in peripheral chambers and explored for 5 minutes. A sex-matched conspecific
127 was then placed under one cup, and the same mouse explored for 5 more minutes. Time
128 spent in the social chamber was video-tracked (TopScan Lite, CleverSys) to assess stress
129 phenotype. Classification was based on the average social chamber time of controls (both
130 D1- and A2A-Cre-RT controls; ~144s). Mice spending <144s were classified as low social
131 interactors while ≥144s were classified as high social interactors. One-way ANOVA with
132 Tukey's post hoc test assessed stress group effects.

133 **Tissue collection & RNA isolation**

134 24h after social interaction testing at 9:00-14:00 ZT, four 14 gauge punches containing the
135 entire NAc that includes both core and shell were collected from D1-Cre-RT and A2A-Cre-RT
136 mice and snap frozen at -80C. Polyribosomes were immunoprecipitated as previously
137 described [25], each sample pooled from four mice with similar SI ratios. Homogenates were
138 incubated with 5 µl anti-HA antibody (Biolegend 901515) at 4°C overnight with rotation.
139 Samples were then incubated with 400 uL of protein G magnetic beads (Life Technologies,
140 Carlsbad, CA, USA #100.09D) overnight at 4°C with rotation. Beads were washed in a
141 magnetic rack with high-salt buffer. RNA was extracted with a DNase step (Qiagen,
142 Germantown, MD, USA) using the RNeasy mini kit (qiagen) by adding RLT and following
143 manufacturer instructions. RNA concentration and quality were assessed via Bioanalyzer
144 (Agilent).

145 **Library preparation and analysis**

146 Samples with RNA integrity number >8 were used and pooled into biological quintuplicates
147 for sequencing at the Maryland Genomics core of the UMSOM Institute for Genome
148 Sciences (IGS) and processed as described previously [26]. Libraries were prepared from
149 10 ng of RNA from each sample using the SMART-Seq v4 kit (Takara). Samples were
150 sequenced using NovaSeq6000 with 100 bp paired-end reads. Reads were aligned to the
151 mouse genome (Mus musculus, GRCm38) using HISAT2 and counted in coding regions using
152 HTSeq (GEO: GSE315159).

153 We used two approaches to characterize transcriptomic alterations. First, edgeR's likelihood
154 ratio test identified DEGs by stress group in MSN subtypes. Genes with False Discovery Rate
155 (FDR) < 0.05 were considered differentially expressed. Gene Ontology (GO) enrichment was
156 performed using R packages 'gprofiler2' and 'clusterProfiler' and the online tool 'DAVID'. We
157 next used weighted gene co-expression network analysis (WGCNA) to identify networks of
158 co-expressed genes in D1- and D2-MSNs. 'blockwiseModules()' identified signed modules
159 using biweight midcorrelation, power = 12, and minimum module size = 25. Module
160 membership scores were calculated by correlating gene expression with module eigengene.
161 Hub genes were defined as those with highest membership scores. Using the R package
162 'limma', differentially regulated modules were identified using module eigengenes in a linear
163 model comparing stress groups. Significant modules were characterized using the same
164 enrichment tools.

165 WGCNA modules were classified into four categories based on hub gene properties and
166 enrichment terms: structural, synaptic, protein synthesis and mitochondrial. Modules
167 dominated by genes and terms linked to morphogenesis, junction/projection formation,
168 cytoskeletal dynamics and ECM interactions were classified as structural. Modules with
169 genes and terms heavily involved in synaptic response, receptor trafficking and signal

170 transduction were classified as synaptic. Protein synthesis modules were composed of
171 genes encoding ribosomal and proteasomal subunits, transcription factors and elongation
172 factors and genes involved in protein processing. Finally, mitochondrial modules were
173 largely composed of respiratory complex components. In cases where properties of
174 modules overlapped between multiple categories, modules were classified into the group
175 that most closely aligned with the properties of modular hub genes.

176 RNA-seq data from male D1- and D2-Cre-RiboTag mice and human male and female NAc
177 postmortem tissue were obtained from GEO [23, 27]. Male mouse reads were downloaded
178 and processed using RSubread (GRCm39); human read counts were downloaded
179 processed.

180 **Consensus module detection and analysis**

181 Human genes were mapped to mouse orthologs using the R package 'orthogene'. Genes
182 with low counts were filtered using edgeR's *filterByExpr*, and normalization used variance
183 stabilizing transformation. Consensus modules were constructed using all datasets (power
184 = 8 and minimum module size = 30). 'Limma' identified differentially regulated modules in
185 each dataset.

186

187 ***Results***

188 ***Social stress in females induces differentially enriched translatomes in nucleus***
189 ***accumbens neuron subtypes***

190 Female D1-Cre-RT and A2A-Cre-RT mice underwent 10 days of CWDS and three chamber
191 social interaction test on day 11 (Fig 1A). High- and low-social interactors (SI) were
192 classified based on control mice's average time in the social chamber (~144 s). This
193 approach captures the natural range of social behavior exhibited by animals and enables
194 comparison across groups. ANOVA confirmed significant differences in interactions times
195 between stress groups (D1: p-value < 0.05, F(2,57) = 45.09; A2A: p-value < 0.05, F(2,58) =
196 25.12, Fig 1B). On day 12 NAc tissue was isolated, HA-tagged polyribosomes
197 immunoprecipitated from D1- or A2A-MSNs, and ribosome-associated RNA isolated and
198 sequenced.

199 We found 9 differentially expressed genes (DEGs) in D1-MSN and 630 in A2A-MSN across
200 stress groups (FDR < 0.05, Fig 1C, Fig S1A-B, Table S1). Seven D1-MSN DEGs differ
201 between high and low SI, with one downregulated in low SI (Fig 1C, top & far right). The top
202 three upregulated genes – *Lars2, Abcc9* and *Kcnj8* -participate in cellular responses to
203 energy deficiency, including an ATP-sensitive inward-rectifying potassium (KATP) channel.

Other upregulated genes are involved in adhesion/migration. Enrichment analysis of upregulated low vs high SI female D1-MSN DEGs include terms such as “ATPase-coupled transmembrane transporter activity” and “potassium import across membrane” while downregulated DEGs are involved in ion transport (Fig 1D). Enrichment analysis also indicates increased expression of genes involved in translation in high SI females and DNA damage response in low SI mice (Table S2).

Due to the low D1-MSN DEG count, enrichment analysis was repeated using a nominal p-value 0.05 cut-off. Low SI upregulated D1-MSN genes are enriched for chromatin- and synapse-related terms; downregulated genes are enriched for apoptosis. High SI D1-MSN upregulated genes are enriched for translation and mitochondrial/respiration terms; downregulated genes involve structural development (Table S1, S3).

A2A-MSNs had more DEGs. In low-SI vs. control/high-SI females, upregulated genes were linked to junction formation, while downregulated genes were involved in synaptic transmission, particularly GPCR signaling (Fig 1C, bottom). In high SI vs control, two ribosomal subunit pseudogenes were differentially regulated. Enrichment analysis showed upregulated genes in low-SI mice were associated with structural development and transcription regulation (Fig 1E, Table S2). Downregulated genes in low SI vs control/high SI genes were enriched for synaptic processes, notably GPCR signaling (Fig 1E). Enrichment analysis using a nominal p-value cutoff produced similar results for all comparisons (Table S3). There is little correlation between the MSN subtypes in gene expression change (Fig S1C).

Female social stress results in altered gene networks in nucleus accumbens neuron subtypes

Weighted Gene Co-expression Network Analysis (WGCNA) of female D1- and A2A-Cre-RT transcriptomes identified 43 D1-MSN and 21 A2A-MSN modules (Fig. 2A-B, 3A-B, S2A-B, Table S4), containing between 33–3263 and 131–3064 genes, respectively (Fig. 2C, 3C). 9 D1-MSN and 5 A2A-MSN modules were significantly associated with high- or low-social interaction (Fig. 2B-C, 3B-C, Table S4). Given that the samples were pooled, we constructed boxplots using the eigengenes of the significant modules across pooled samples to examine potential sources of variability. Our results for both the D1- and A2A-Cre-RT modules indicate that module score medians all center around 0 with similar interquartile ranges. Eigengene variability doesn’t indicate any kind of instability across pools and there is no indication of any individual pooled sample driving eigengene signal (Fig S3, S4).

The significant modules were characterized as described in the methods and placed into four categories: structural processes, protein synthesis, synapse/signaling and

240 mitochondria related (Fig 2D, 3D, Table S5). WGCNA was also applied to chronically
241 stressed male MSN subtypes and human NAc MDD datasets, identifying seven D1- and
242 one A2A-MSN module associated with social interaction, and 12 human NAc modules
243 significant by sex, condition, or both (Fig S3-S5, Table S6-9) [27].

244 Significant modules across female stress groups highlight the diverse effects of chronic
245 social stress on MSN transcriptomes. While both female SI groups show differential
246 regulation in D1-MSN modules, A2A-MSN modules are primarily affected in low SI females
247 (Fig 2B, 3B). In contrast, male CSDS data show D1-MSN modules primarily impacted in low
248 SI mice with one A2A-MSN module upregulated in both stress groups (Fig S5B, Fig S7B)
249 [27]. Module preservation analysis demonstrated a lack of preservation between male and
250 female mice, pointing to sex-specific transcriptional network architecture in these neurons
251 and indicating that chronic stress impact distinct molecular mechanisms by sex (Fig S6,
252 S8). This could also be indicative to the different types of stress- physical vs. emotional-
253 and future studies are warranted to better understand these differences."

254 Protein turnover modules, F D1 M20 and F A2A M3, are downregulated in low vs high SI (Fig
255 2D, 3D). F D1 M20 hub genes regulate transcription elongation, RNA degradation, and
256 cytoskeletal dynamics, whereas F A2A M3 hub genes involve tRNA loading, RNA splicing,
257 and cell adhesion (Fig 2D, 3D, Table S4). Enrichment results support these findings, with F
258 D1 M20 genes enriched for elongation, ribosome, and proteasome terms, and F A2A M3
259 genes for localization and transport terms (Table S5). Multiple significant female modules
260 highlight modulatory processes in protein synthesis and transport. The F D1 M28 module,
261 downregulated in high SI vs controls, includes ribosomal subunit pseudogenes and stress
262 response genes, (such as Rgs2, Manf, Isg15), suggesting ribosomal dysfunction (Fig 2D,
263 Table S4-5). F D1 M36 is enriched for transcription regulation, Golgi function and RNA
264 polymerase II activity while the F A2A M6 module is enriched for RNA polymerase II activity
265 and ER-related terms (Fig 2D, 3D, Table S5). F D1 M36 is downregulated in high SI vs
266 control, whereas F A2A M6 is upregulated in low vs high SI mice (Fig 2D, 3D). These results
267 indicate reduced regulatory protein processes in D1-MSN of high SI females, but increased
268 transcriptional regulation in A2A-MSNs of low SI females.

269 Structural regulation modules are exclusive to D1-MSNs. The F D1 M12 module,
270 upregulated in low SI, includes hub genes involved in adhesion/migration, GPCR signaling,
271 and stress response, with enrichment terms involving adhesion/migration and cytokine
272 activity (Fig 2D, Table S5). Another low SI-upregulated module, F D1 M35, includes hub
273 genes and enriched terms linked to dendrite organization and adhesion (Fig 2D, Table S5).
274 In contrast, F D1 M31, downregulated in high SI, features genes enriched for
275 cytoskeletal/membrane-related terms and hub genes in lipid trafficking, cytoskeletal
276 organization, and growth factor signaling, suggesting transcriptional activity directed

towards regulating structural processes (Fig 2D, Table S5). A similar male module, M D1 M22, is upregulated in low SI males, suggesting sex differences (Fig S5D, Table S6-7) [27]. These findings indicate increased neurite-forming activity in low SI females and reduced structural maintenance in high SI females.

Two D1- and three A2A-MSN modules include genes heavily involved in synaptic function. F D1 M40, downregulated low vs high SI and upregulated high SI vs controls, includes hub genes linked to synaptic vesicle sorting and release, with enrichment for protein processing- and transport-related terms (Fig 2D, Table S4-5). Similarly, F A2A M15, downregulated in low SI, includes genes involved in neurotransmitter/ neuropeptide vesicle release, with enrichment for terms involving protein localization and secretory granules (Fig 3D, Table S5). These results suggest reduced synaptic activity in low SI females across both subtypes, while increased D1-MSN synaptic activity is associated with high SI. The male module M D1 M10, also synaptic-related, is upregulated low SI vs control but downregulated in low SI vs high SI (Fig S5D, Table S6-7) [27]. F A2A M10, downregulated low SI vs controls/high SI, includes hub genes encoding receptors and components of receptor-mediated signal transduction. Enrichment results show significant association with terms involved in synaptic transmission and signal transduction (Fig 3D, Table S4-5). The male module M D2 M20 likewise includes genes involved in synaptic transduction however is upregulated in both low SI and high SI compared to control (Fig S7D) [27]. Overall, increased expression of genes involved in synaptic activity in D1-MSN correlates with high sociability in both sexes, with sex differences in genes involved in A2A-MSN synaptic input.

Other significant synaptic modules include genes involved in synaptic maintenance. F D1 M41, linked to synaptic structural integrity and transport, is upregulated low vs high SI/controls (Fig 2D, Table S5). F A2A M5 includes hub genes involved in vesicle trafficking, encoding receptors/channels as well as synaptic structure formation (Fig 3D, Table S4-5). This module is also upregulated low SI vs controls, suggesting that genes involved in distinct aspects of synaptic maintenance are upregulated in low SI female mice by MSN subtype. In contrast, male modules that include genes involved in synaptic maintenance, M D1 M34 and M D1 M36, are downregulated low SI vs control (Fig S5D, Table S6-7) [27]. These results suggest that the regulation/modulation of synaptic activity may underlie sex differences.

F D1 M18 module, upregulated high SI vs control and downregulated low SI vs high SI, includes genes encoding mitochondrial respiratory chain and ribosomal (cytoplasmic and mitochondrial) subunits (Fig 2D, Table S4-5). F A2A M3 contains transcriptional/mitochondrial genes (Fig 3D, Table S4). These results indicate reduced

mitochondrial activity in low SI D1-MSNs, with possible sex differences across MSN subtypes.

In human MDD WGCNA results, modules containing genes involved in synaptic transmission and regulation are upregulated in female controls, while a module with genes involved in synaptic development is downregulated relative to males. In MDD, synaptic development is downregulated in females. Mitochondrial and immune/inflammatory modules are upregulated in females in both control and MDD groups (Fig S9, Table S8-9).

Female D1- and A2A-MSN modules with highest DEG proportions share common regulatory components

Modules with highest DEG proportions were selected for analysis. F D1 M12, upregulated low vs high SI, includes adhesion and cell-matrix interaction hub genes (Fig 4A, Table S4-5). DEGs include Vtn, KATP channel genes, and Lars2, all upregulated in low vs high SI. F A2A M10, downregulated low SI, includes downregulated DEGs involved in synaptic signaling (Fig 4B, Table S4-5). Enrichment analysis links both modules to PI3K-Akt-mTOR signaling (Fig 4C). Genes with high membership scores were analyzed for transcriptional regulation (Fig 4D). Nf1 and Klf6 emerged as key regulators. Nf1-regulated D1 M12 genes are linked to migration and growth factor signaling, A2A M10 genes to synaptic functions (Fig 4E).

Cross species consensus modules

Consensus module analysis was performed using the female CWDS dataset, male CSDS and human MDD datasets [23, 27]. 4029 genes overlapped across processed datasets (Fig 5A,B, Table S10). After module construction, relationship to experimental groups was assessed. One module, module 3, is differentially regulated across mice and humans (Fig 5C-E). Boxplots using the consensus module eigengenes indicate that module score medians all center around 0 for across all datasets with similar interquartile ranges (Fig S10). Hub genes involve transcription regulation and PI3K/Akt signaling (Table S10). Enrichment analysis shows that the module is involved in transport and synaptic development as well as inositol phosphate activity (Fig 5E, Table S11). Positive module score genes are enriched for synaptic activity and phosphatidylinositol-mediated signaling; negative module score genes for structural and translation terms.

Discussion

We investigated sex-specific effects of chronic social stress on NAc MSN subtype transcriptomes. Using female D1-Cre-RT and A2A-Cre-RT mice exposed to CWDS, we identified unique DEGs and co-expression networks linked to social interaction phenotype, as well as networks showing sex-specific regulation in mice and humans. Genes

upregulated in D1-MSNs of low-SI females suggest altered respiratory activity. Two encode ATP-sensitive potassium channels (KATP), which regulate excitability based on ATP levels, and *Lars2* encodes a mitochondrial aminoacyl-tRNA synthetase. KATP expression increases under hypoxia, while altered mt-aaRS expression is linked to mitochondrial dysfunction [28, 29]. These findings align with mitochondrial changes in D1-MSNs associated with depressive-like behavior and social deficits [30, 31]. Together, the DEGs and module results suggest mitochondrial dysfunction contributes to low SI in females, while mitochondrial genes and biogenesis are increased in high SI females. WGCNA also shows downregulation of co-expression networks for energy-demanding processes like protein synthesis, transport, and synaptic release in low-SI D1-MSNs. A recent study found that chronic dietary supplementation of urolithin A, a gut metabolite known to enhance mitochondrial health, produces anxiolytic effects in high anxiety mice mediated by the reversal of dysfunctional mitochondrial mechanisms in the MSNs of NAc [40]. Given the high degree of comorbidity between anxiety disorders and mood disorders, these results suggest that targeting mitochondria in MSN subtypes may produce therapeutic effects.

There were far more DEGs in female A2A-MSNs relative to D1-MSNs. In low-SI females, top upregulated A2A-MSN genes are involved in structure and transcription, while top downregulated genes relate to synaptic activity, consistent with enrichment analysis results. Our previous studies observed male low-SI mice display increased frequency of excitatory input and number of thin and stubby spines on A2A-MSNs [30, 32]. This suggest sex differences A2A-MSN synaptic activity, with reduced activity in low-SI females potentially driving stress susceptibility. Supporting this, WGCNA identified multiple A2A-MSN gene co-expression networks impacted by chronic social stress that are composed of genes involved in synaptic processes. Although the modules with genes linked to synaptic input and release are downregulated in low-SI female mice, modules linked to synapse development/formation is upregulated, possibly as a compensatory or adaptive mechanism.

We identified sex differences by comparing female CWDS results with male CSDS modules [27]. In D1-MSNs, differences were observed in structural regulation modules: F D1 M31 is downregulated in high SI females, whereas M D1 M22 is upregulated in low SI males. Both modules include genes involved in cytoskeletal regulation and lipid processing; however, F D1 M31 genes involve growth factor signaling, whereas M D1 M22 genes involve lipid processing. These results suggest stress may impair growth factor–dependent cytoskeletal remodeling in females, limiting dendritic expansion and plasticity, while in males, altered lipid metabolism may affect membrane composition and spine stability. In A2A-MSNs, there are differences in genes involved in synaptic input. F A2A M10 is downregulated in low SI vs control/high-SI females while M D2 M20 is upregulated in low-

385 SI males. Although only a few genes overlap, hub genes in both regulate GPCR signaling,
386 vesicle transport, and cytoskeletal dynamics. Sex differences in MSN morphology and
387 connectivity have been reported; though the mechanism remains unclear [33]. These
388 results suggest stress susceptibility may be the result of opposing transcriptional
389 trajectories: reduced GPCR activity produces dampened response in low-SI female A2A-
390 MSNs, while male low-SI A2A-MSNs may experience enhanced maladaptive excitatory
391 signaling. Further research is needed to clarify A2A-MSN input alterations.

392 In D1-MSNs, the D1 M12 module contains the highest proportion of DEGs, with
393 upregulation in low vs high SI groups. Multiple hub genes encode proteins involved in
394 migration. Vitronectin, a glycoprotein regulating cell adhesion and migration, is
395 upregulated in low SI females [34]. Other hub genes are involved in GPCR signaling and
396 homeostasis. Stress-induced depressive behaviors are linked to D1-MSN dendritic atrophy
397 via GTPase RhoA upregulation [32]. Given its involvement in GPCR signaling and
398 cytoskeletal regulation, D1 M12 likely contributes to this atrophy in low-SI mice.

399 Among A2A-MSN modules, A2A M10 had the highest proportion of DEGs. Its hub
400 genes, involved in synaptic and GPCR signaling, include *Oxtr* and *Resp18*, both
401 downregulated in low-SI mice, suggesting reduced peptidergic signaling [35]. *Oxtr* encodes
402 the oxytocin receptor, linked to social reward and expressed in both D1- and A2A-MSNs
403 [36]. All low vs. high SI DEGs in A2A M10 were downregulated and enriched for synaptic
404 terms. The module itself was downregulated in low-SI vs. controls and high-SI females.
405 Prior studies show increased excitatory input onto A2A-MSNs in low-SI mice post-defeat
406 [20], suggesting reduced A2A M10 activity reflects weakened modulatory synaptic input.

407 Enrichment analysis revealed that both D1 M12 and A2A M10, oppositely regulated
408 in low SI, are significantly enriched for the PI3K-Akt pathway, involved in cell growth and
409 survival [37]. It also plays a neuroprotective role under cellular stress [38]. The PI3K-Akt
410 genes in D1 M12 are associated with the MAPK/ERK pathway. Dendrite morphogenesis
411 involves both the PI3K and the MAPK pathway, and PI3K-dependent dendritic remodeling
412 plays a neuroprotective role [39, 41]. The D2 M10 genes linked to PI3K/Akt center on
413 synaptic signal transduction. This is consistent with previous studies which have
414 established that the PI3K/Akt pathway is involved in various components of synaptic
415 activity [37].

416 Consensus module analysis of the female CWDS, male CSDS, and human MDD
417 datasets identified module 3 as sex-specific in both mice and humans [23, 27]. Results
418 show an upregulation in module 3 activity in the female human NAc at baseline that is
419 significantly reduced in the MDD condition. Additionally, the cell subtype-specific mouse
420 transcriptomes display a reduction in module 3 activity in the A2A-MSN of low SI females.

421 This suggests that module 3 in A2A-MSNs represents a sex-specific mechanism that may
422 be reduced in NAc A2A-MSNs of human females with MDD. Conversely, high SI males show
423 reduced module 3 activity in D1-MSNs, suggesting that the reduction of module 3 activity in
424 D1-MSNs of male mice may be protective. Further work is required to determine whether
425 baseline sex differences in MSN subtypes drive sex- and subtype-specific PI3K-Akt
426 responses. Hub genes in this module regulate transcription and PI3K-Akt signaling, while
427 enrichment analysis indicates involvement in mTOR signaling, downstream of PI3K-Akt.
428 Abnormal PI3K-Akt pathway activity in the NAc is linked to multiple substance use
429 disorders [42-44]. Some studies suggest sex-specific involvement in the NAc [45-46]. A
430 recent study investigating ketamine's anti-depressant effects observed sex-specific AKT-
431 mTOR signaling alterations in the hippocampus; decreased activity in males linked to
432 memory impairment, increased activity in females linked to resilience [47]. Although
433 further research is required, our findings suggest PI3K/Akt signaling is involved in the sex-
434 specific stress response in the NAc in a subtype-specific manner.

435 iRegulon analysis identified key transcriptional regulators, notably NF1
436 (Neurofibromin 1), as a shared regulator of F D1 M12 and F A2A M10 modules (Fig 4D). NF1,
437 a tumor suppressor, influences migration, cytoskeletal dynamics, and stress responses
438 through pathways including Ras/MAPK, Raf/MEK/ERK, PI3K/AKT/mTOR, and cAMP/PKA (Fig
439 4E) [48]. It also contributes to reward and motor behavior via its role in D1- and A2A-MSNs
440 and is linked to striatal neuropsychiatric conditions [49-50]. NF1 may act as a signaling hub
441 for GPCR pathways and could mediate stress-induced effects on MSN subtypes via
442 PI3K/AKT/mTOR signaling.

443 There were a few limitations to the study. To begin with, there was a small number of
444 DEGs identified in the D1-MSN of female mice. This may have been the result of using
445 RiboTag-based approach which may yield more conservative DEG profiles compared to
446 total RNA-seq. Additionally, the pooling of animals may have limited the estimation of inter-
447 individual variance, which could have reduced the power to detect subtle differential
448 expression. Moreover, estrous cycle stage was not assessed, limiting our ability to
449 determine how fluctuations in ovarian hormones such as estrogen may influence nucleus
450 accumbens translatomic profiles in female mice [51-52]. Future studies incorporating
451 estrous cycle staging will be important for disentangling hormone-dependent
452 transcriptional mechanisms underlying stress phenotype in females. In addition to this,
453 due to the lack of available transcriptomic data from male mice performing CWDS, our
454 consensus module analysis relied on male CSDS data. Although the difference in stress
455 type may influence outcomes, both paradigms involve social stress but differ in physical
456 versus vicarious exposure. Given that the purpose of WGCNA is to find conserved networks
457 and test how they differ by stress and sex, our results allow us to examine both conserved

and paradigm-specific transcriptional modules. Future studies should examine the transcriptomic alterations induced in MSN subtypes by CSDS, including newly developed female models, relative to CWDS, to investigate how different forms of stress contribute to MDD onset. In addition to this, further work will be needed to experimentally validate stress-associated genes and network-level signatures identified in this study using targeted molecular approaches. An important aspect of our study is the analysis of female subjects, extending beyond prior transcriptomic studies that focused solely on males [53 – 55].

In conclusion, chronic stress affects MSN subtypes in a cell-type- and sex-specific manner. Morphological, synaptic, mitochondrial, and transcriptional changes contribute to female vulnerability, potentially driven by PI3K/Akt/mTOR signaling and NF1. By identifying sex-specific molecular signatures in NAc MSN subtypes after social stress, this study offers key insights into MDD mechanisms and highlights potential targets for sex-informed therapies.

References

1. Bains, Navneet, and Sara Abdijadid. “Major Depressive Disorder.” In *StatPearls*. Treasure Island (FL): StatPearls Publishing, 2025. http://www.ncbi.nlm.nih.gov/books/NBK559078/.
2. Severe, Jennifer, John F. Greden, and Priyanka Reddy. “Consequences of Recurrence of Major Depressive Disorder: Is Stopping Effective Antidepressant Medications Ever Safe?” *Focus* 18, no. 2 (April 2020): 120–28. https://doi.org/10.1176/appi.focus.20200008.
3. Berton, Olivier, Colleen A. McClung, Ralph J. Dileone, Vaishnav Krishnan, William Renthal, Scott J. Russo, Danielle Graham, et al. “Essential Role of BDNF in the Mesolimbic Dopamine Pathway in Social Defeat Stress.” *Science (New York, N.Y.)* 311, no. 5762 (February 10, 2006): 864–68. https://doi.org/10.1126/science.1120972.
4. Krishnan, Vaishnav, Ming-Hu Han, Danielle L. Graham, Olivier Berton, William Renthal, Scott J. Russo, Quincey Laplant, et al. “Molecular Adaptations Underlying Susceptibility and Resistance to Social Defeat in Brain Reward Regions.” *Cell* 131, no. 2 (October 19, 2007): 391–404. https://doi.org/10.1016/j.cell.2007.09.018.
5. Krishnan, Vaishnav, and Eric J. Nestler. “Linking Molecules to Mood: New Insight into the Biology of Depression.” *The American Journal of Psychiatry* 167, no. 11 (November 2010): 1305–20. https://doi.org/10.1176/appi.ajp.2009.10030434.
6. Sial, Omar K., Brandon L. Warren, Lyonna F. Alcantara, Eric M. Parise, and Carlos A. Bolaños-Guzmán. “Vicarious Social Defeat Stress: Bridging the Gap between Physical

and Emotional Stress." *Journal of Neuroscience Methods* 258 (January 30, 2016): 94–103. https://doi.org/10.1016/j.jneumeth.2015.10.012.

7. Francis, T. Chase, and Mary Kay Lobo. "Emerging Role for Nucleus Accumbens Medium Spiny Neuron Subtypes in Depression." *Biological Psychiatry* 81, no. 8 (April 15, 2017): 645–53. https://doi.org/10.1016/j.biopsych.2016.09.007.
8. Iñiguez, Sergio D., Francisco J. Flores-Ramirez, Lace M. Riggs, Jason B. Alipio, Israel Garcia-Carachure, Mirella A. Hernandez, David O. Sanchez, et al. "Vicarious Social Defeat Stress Induces Depression-Related Outcomes in Female Mice." *Biological Psychiatry* 83, no. 1 (January 1, 2018): 9–17. https://doi.org/10.1016/j.biopsych.2017.07.014.
9. Patel, Deepika, Martien J. Kas, Sumantra Chattarji, and Bauke Buwalda. "Rodent Models of Social Stress and Neuronal Plasticity: Relevance to Depressive-like Disorders." *Behavioural Brain Research* 369 (September 2, 2019): 111900. https://doi.org/10.1016/j.bbr.2019.111900.
10. Seney, Marianne L., Jill Glausier, and Etienne Sibille. "Large-Scale Transcriptomics Studies Provide Insight Into Sex Differences in Depression." *Biological Psychiatry*, Insight Into Sex Differences in Psychiatric Syndromes From Transcriptomic Analyses, 91, no. 1 (January 1, 2022): 14–24. https://doi.org/10.1016/j.biopsych.2020.12.025.
11. Franco, Daniela, Andreas B. Wulff, Mary Kay Lobo, and Megan E. Fox. "Chronic Physical and Vicarious Psychosocial Stress Alter Fentanyl Consumption and Nucleus Accumbens Rho GTPases in Male and Female C57BL/6 Mice." *Frontiers in Behavioral Neuroscience* 16 (February 10, 2022): 821080. https://doi.org/10.3389/fnbeh.2022.821080.
12. Newman EL, Covington HE 3rd, Suh J, Bicakci MB, Ressler KJ, DeBold JF, Miczek KA. Fighting Females: Neural and Behavioral Consequences of Social Defeat Stress in Female Mice. Biol Psychiatry. 2019 Nov 1;86(9):657-668. https://doi.org/10.1016/j.biopsych.2019.05.005.
13. Harris AZ, Atsak P, Bretton ZH, Holt ES, Alam R, Morton MP, Abbas AI, Leonardo ED, Bolkan SS, Hen R, Gordon JA. A Novel Method for Chronic Social Defeat Stress in Female Mice. Neuropsychopharmacology. 2018 May;43(6):1276-1283. https://doi.org/10.1038/npp.2017.259.
14. Takahashi A, Chung JR, Zhang S, Zhang H, Grossman Y, Aleyasin H, Flanigan ME, Pfau ML, Menard C, Dumitriu D, Hodes GE, McEwen BS, Nestler EJ, Han MH, Russo SJ. Establishment of a repeated social defeat stress model in female mice. Sci Rep. 2017 Oct 9;7(1):12838. https://doi.org/10.1038/s41598-017-12811-8.
15. Nestler, Eric J. "Role of the Brain's Reward Circuitry in Depression: Transcriptional Mechanisms." *International Review of Neurobiology* 124 (2015): 151–70. https://doi.org/10.1016/bs.irn.2015.07.003.

16. Fox, Megan E., and Mary Kay Lobo. “The Molecular and Cellular Mechanisms of Depression: A Focus on Reward Circuitry.” *Molecular Psychiatry* 24, no. 12 (December 2019): 1798–1815. https://doi.org/10.1038/s41380-019-0415-3.
17. Ding, Yu-Dan, Xiao Chen, Zuo-Bing Chen, Le Li, Xue-Ying Li, Francisco Xavier Castellanos, Tong-Jian Bai, et al. “Reduced Nucleus Accumbens Functional Connectivity in Reward Network and Default Mode Network in Patients with Recurrent Major Depressive Disorder.” *Translational Psychiatry* 12 (June 6, 2022): 236. https://doi.org/10.1038/s41398-022-01995-x.
18. Gerfen, Charles R., Keefe, Kristen A. Neostriatal dopamine receptors. Trends Neurosci. 1994 Jan;17(1):2-3: 7511845. doi: https://doi.org/10.1016/0166-2236(94)90022-1.
19. Smith RJ, Lobo MK, Spencer S, Kalivas PW. Cocaine-induced adaptations in D1 and D2 accumbens projection neurons (a dichotomy not necessarily synonymous with direct and indirect pathways). *Current Opinion in Neurobiology* (2013 Aug;23(4)):546-52. https://doi.org/10.1016/j.conb.2013.01.026.
20. Francis, T. Chase, Ramesh Chandra, Danielle M. Friend, Eric Finkel, Genesis Dayrit, Jorge Miranda, Julie M. Brooks, et al. “Nucleus Accumbens Medium Spiny Neuron Subtypes Mediate Depression-Related Outcomes to Social Defeat Stress.” *Biological Psychiatry* 77, no. 3 (February 1, 2015): 212–22. https://doi.org/10.1016/j.biopsych.2014.07.021.
21. Coccurello, Roberto. “Anhedonia in Depression Symptomatology: Appetite Dysregulation and Defective Brain Reward Processing.” *Behavioural Brain Research* 372 (October 17, 2019): 112041. https://doi.org/10.1016/j.bbr.2019.112041.
22. Kim, Hee-Dae, Jing Wei, Tanessa Call, Xiaokuang Ma, Nicole Teru Quintus, Alexander J. Summers, Samantha Carotenuto, et al. “SIRT1 Coordinates Transcriptional Regulation of Neural Activity and Modulates Depression-Like Behaviors in the Nucleus Accumbens.” *Biological Psychiatry*, Depression Dimensions and Subtypes, 96, no. 6 (September 15, 2024): 495–505. https://doi.org/10.1016/j.biopsych.2024.03.017.
23. Labonté, Benoit, Olivia Engmann, Immanuel Purushothaman, Caroline Menard, Junshi Wang, Chunfeng Tan, Joseph R Scarpa, et al. “Sex-Specific Transcriptional Signatures in Human Depression.” *Nature Medicine* 23, no. 9 (September 2017): 1102–11. https://doi.org/10.1038/nm.4386.
24. Sanz, Elisenda, Linghai Yang, Thomas Su, David R. Morris, G. Stanley McKnight, and Paul S. Amieux. “Cell-Type-Specific Isolation of Ribosome-Associated mRNA from Complex Tissues.” *Proceedings of the National Academy of Sciences* 106, no. 33 (August 18, 2009): 13939–44. https://doi.org/10.1073/pnas.0907143106.
25. Fox, Megan E., Andreas B. Wulff, Daniela Franco, Eric Y. Choi, Cali A. Calarco, Michel Engeln, Makeda D. Turner, et al. “Adaptations in Nucleus Accumbens Neuron Subtypes Mediate Negative Affective Behaviors in Fentanyl Abstinence.” *Biological Psychiatry*,

Addiction Phenotypes and Mechanisms, 93, no. 6 (March 15, 2023): 489–501. https://doi.org/10.1016/j.biopsych.2022.08.023.

26. Engeln, Michel, Yang Song, Ramesh Chandra, Ashley La, Megan E. Fox, Brianna Evans, Makeda D. Turner, et al. "Individual Differences in Stereotypy and Neuron Subtype Translatome with TrkB Deletion." *Molecular Psychiatry* 26, no. 6 (June 2021): 1846–59. https://doi.org/10.1038/s41380-020-0746-0.
27. Kim, Hee-Dae, Jing Wei, Tanessa Call, Nicole Teru Quintus, Alexander J. Summers, Samantha Carotenuto, Ross Johnson, et al. "Shisa6 Mediates Cell-Type Specific Regulation of Depression in the Nucleus Accumbens." *Molecular Psychiatry* 26, no. 12 (December 2021): 7316–27. https://doi.org/10.1038/s41380-021-01217-8.
28. Soundarapandian, Mangala M., Xiaofen Zhong, Lisheng Peng, Di Wu, and Youming Lu. "Role of KATP Channels in Protection against Neuronal Excitatory Insults." *Journal of Neurochemistry* 103, no. 5 (2007): 1721–29. https://doi.org/10.1111/j.1471-4159.2007.04963.x.
29. Sissler, Marie, Ligia Elena González-Serrano, and Eric Westhof. "Recent Advances in Mitochondrial Aminoacyl-tRNA Synthetases and Disease." *Trends in Molecular Medicine* 23, no. 8 (August 1, 2017): 693–708. https://doi.org/10.1016/j.molmed.2017.06.002.
30. Gebara, Elias, Olivia Zanoletti, Sriparna Ghosal, Jocelyn Grosse, Bernard L. Schneider, Graham Knott, Simone Astori, and Carmen Sandi. "Mitofusin-2 in the Nucleus Accumbens Regulates Anxiety and Depression-like Behaviors Through Mitochondrial and Neuronal Actions." *Biological Psychiatry* 89, no. 11 (June 1, 2021): 1033–44. https://doi.org/10.1016/j.biopsych.2020.12.003.
31. Hollis, Fiona, Michael A. van der Kooij, Olivia Zanoletti, Laura Lozano, Carles Cantó, and Carmen Sandi. "Mitochondrial Function in the Brain Links Anxiety with Social Subordination." *Proceedings of the National Academy of Sciences* 112, no. 50 (December 15, 2015): 15486–91. https://doi.org/10.1073/pnas.1512653112.
32. Fox, Megan E., Ramesh Chandra, Miriam S. Menken, Emily J Larkin, Hyungwoo Nam, Michel Engeln, T. Chase Francis, and Mary Kay Lobo. "Dendritic Remodeling of D1 Neurons by RhoA/Rho-Kinase Mediates Depression-like Behavior." *Molecular Psychiatry* 25, no. 5 (May 2020): 1022–34. https://doi.org/10.1038/s41380-018-0211-5.
33. Forlano, Paul M., and Catherine S. Woolley. "Quantitative Analysis of Pre- and Postsynaptic Sex Differences in the Nucleus Accumbens." *The Journal of Comparative Neurology* 518, no. 8 (April 15, 2010): 1330–48. https://doi.org/10.1002/cne.22279.
34. Ruzha, Yelizhati, Junjun Ni, Zhenzhen Quan, Hui Li, and Hong Qing. "Role of Vitronectin and Its Receptors in Neuronal Function and Neurodegenerative Diseases." *International Journal of Molecular Sciences* 23, no. 20 (October 16, 2022): 12387. https://doi.org/10.3390/ijms232012387.

35. Atari, Ealla, Mitchel C Perry, Pedro A Jose, and Sivarajan Kumarasamy. “Regulated Endocrine-Specific Protein-18, an Emerging Endocrine Protein in Physiology: A Literature Review.” *Endocrinology* 160, no. 9 (September 1, 2019): 2093–2100. https://doi.org/10.1210/en.2019-00397.
36. Dölen, Gül, Ayeh Darvishzadeh, Kee Wui Huang, and Robert C. Malenka. “Social Reward Requires Coordinated Activity of Accumbens Oxytocin and 5HT.” *Nature* 501, no. 7466 (September 12, 2013): 179–84. https://doi.org/10.1038/nature12518.
37. Sánchez-Alegría, Karina, Manuel Flores-León, Evangelina Avila-Muñoz, Nelly Rodríguez-Corona, and Clorinda Arias. “PI3K Signaling in Neurons: A Central Node for the Control of Multiple Functions.” *International Journal of Molecular Sciences* 19, no. 12 (December 2018): 3725. https://doi.org/10.3390/ijms19123725.
38. Goyal, Ahsas, Anant Agrawal, Aanchal Verma, and Nandini Dubey. “The PI3K-AKT Pathway: A Plausible Therapeutic Target in Parkinson’s Disease.” *Experimental and Molecular Pathology* 129 (February 1, 2023): 104846. https://doi.org/10.1016/j.yexmp.2022.104846.
39. Kumar, Vikas, Ming-Xiang Zhang, Michael W. Swank, Jeannette Kunz, and Gang-Yi Wu. “Regulation of Dendritic Morphogenesis by Ras–PI3K–Akt–mTOR and Ras–MAPK Signaling Pathways.” *The Journal of Neuroscience* 25, no. 49 (December 7, 2005): 11288–99. https://doi.org/10.1523/JNEUROSCI.2284-05.2005.
40. Mallet, D., Ülgen, D. H., Grosse, J., Zanoletti, O., Guillot de Suduiraut, I., Monzel, A. S., D'Amico, D., Rinsch, C., Picard, M., Astori, S., & Sandi, C. (2025). Urolithin A Abolishes High Anxiety and Rescues the Associated Mitochondria-Related Transcriptomic Signatures and Synaptic Function. *Biological Psychiatry*, S0006-3223(25)01378-2. https://doi.org/10.1016/j.biopsych.2025.07.020
41. Mutti, Veronica, Federica Bono, Zaira Tomasoni, Leonardo Bontempi, Adele Guglielmi, Silvia Bolognin, Jens C. Schwamborn, Cristina Missale, and Chiara Fiorentini. “Structural Plasticity of Dopaminergic Neurons Requires the Activation of the D3R-nAChR Heteromer and the PI3K-ERK1/2/Akt-Induced Expression of c-Fos and p70S6K Signaling Pathway.” *Molecular Neurobiology* 59, no. 4 (2022): 2129–49. https://doi.org/10.1007/s12035-022-02748-z.
42. Neasta, Jérémie, Sami Ben Hamida, Quinn V. Yowell, Sebastien Carnicella, and Dorit Ron. “AKT Signaling Pathway in the Nucleus Accumbens Mediates Excessive Alcohol Drinking Behaviors.” *Biological Psychiatry* 70, no. 6 (September 15, 2011): 575–82. https://doi.org/10.1016/j.biopsych.2011.03.019.
43. Hong, Sa-Ik, Min-Jung Kim, In-Jee You, Seung-Hwan Kwon, Shi-Xun Ma, Ji-Young Hwang, Jee-Yeon Seo, et al. “Phentermine Induces Conditioned Rewarding Effects via Activation of the PI3K/Akt Signaling Pathway in the Nucleus Accumbens.” *Psychopharmacology* 233, no. 8 (April 1, 2016): 1405–13. https://doi.org/10.1007/s00213-016-4231-z.

646 44. Zhu H, Zhuang D, Lou Z, Lai M, Fu D, Hong Q, Liu H, Zhou W. Akt and its phosphorylation
647 in nucleus accumbens mediate heroin-seeking behavior induced by cues in rats. Addict
648 Biol. 2021 Sep;26(5):e13013. https://doi.org/10.1111/adb.13013.
649 45. Cozzoli, Debra K., Moriah N. Kaufman, Michelle A. Nipper, Joel G. Hashimoto, Kristine
650 M. Wiren, and Deborah A. Finn. "Functional Regulation of PI3K-Associated Signaling in
651 the Accumbens by Binge Alcohol Drinking in Male but Not Female Mice."
652 *Neuropharmacology* 105 (June 1, 2016): 164–74.
653 https://doi.org/10.1016/j.neuropharm.2016.01.010.
654 46. Finn, Deborah A., Joel G. Hashimoto, Debra K. Cozzoli, Melinda L. Helms, Michelle A.
655 Nipper, Moriah N. Kaufman, Kristine M. Wiren, and Marina Guizzetti. "Binge Ethanol
656 Drinking Produces Sexually Divergent and Distinct Changes in Nucleus Accumbens
657 Signaling Cascades and Pathways in Adult C57BL/6J Mice." *Frontiers in Genetics* 9
658 (September 10, 2018). https://doi.org/10.3389/fgene.2018.00325.
659 47. Garcia-Carachure I, Lira O, Themann A, Rodriguez M, Flores-Ramirez FJ, Lobo MK,
660 Iñiguez SD. Sex-Specific Alterations in Spatial Memory and Hippocampal AKT-mTOR
661 Signaling in Adult Mice Pre-exposed to Ketamine and/or Psychological Stress During
662 Adolescence. Biol Psychiatry Glob Open Sci. 2023 Aug 10;4(1):240-251.
663 https://doi.org/10.1016/j.bpsgos.2023.07.009.
664 48. Báez-Flores, Juan, Mario Rodríguez-Martín, and Jesus Lacal. "The Therapeutic Potential
665 of Neurofibromin Signaling Pathways and Binding Partners." *Communications Biology* 6
666 (April 20, 2023): 436. https://doi.org/10.1038/s42003-023-04815-0.
667 49. Sutton LP, Muntean BS, Ostrovskaya O, Zucca S, Dao M, et al. (2019) NF1-cAMP
668 signaling dissociates cell type–specific contributions of striatal medium spiny neurons
669 to reward valuation and motor control. PLOS Biology 17(10): e3000477.
670 https://doi.org/10.1371/journal.pbio.3000477.
671 50. Xie K, Colgan LA, Dao MT, Muntean BS, Sutton LP, Orlandi C, et al. NF1 Is a Direct G
672 Protein Effector Essential for Opioid Signaling to Ras in the Striatum. Curr Biol. 2016;
673 26(22):2992–3003. https://doi.org/10.1016/j.cub.2016.09.010.
674 51. Proaño, S. B., Morris, H. J., Kunz, L. M., Dorris, D. M., & Meitzen, J. (2018). Estrous cycle-
675 induced sex differences in medium spiny neuron excitatory synaptic transmission and
676 intrinsic excitability in adult rat nucleus accumbens core. *Journal of*
677 *neurophysiology*, *120*(3), 1356–1373. https://doi.org/10.1152/jn.00263.2018
678 52. Rocks, D., Cham, H., & Kundakovic, M. (2022). Why the estrous cycle matters for
679 neuroscience. *Biology of sex differences*, *13*(1), 62. https://doi.org/10.1186/s13293-
680 022-00466-8
681 53. Peña CJ, Kronman HG, Walker DM, Cates HM, Bagot RC, Purushothaman I, Issler O, Loh
682 YE, Leong T, Kiraly DD, Goodman E, Neve RL, Shen L, Nestler EJ. Early life stress confers

683 lifelong stress susceptibility in mice via ventral tegmental area OTX2. Science. 2017 Jun
684 16;356(6343):1185-1188. https://doi.org/10.1126/science.aan4491.
685 54. Bagot RC, Cates HM, Purushothaman I, Lorsch ZS, Walker DM, Wang J, Huang X,
686 Schlüter OM, Maze I, Peña CJ, Heller EA, Issler O, Wang M, Song WM, Stein JL, Liu X,
687 Doyle MA, Scobie KN, Sun HS, Neve RL, Geschwind D, Dong Y, Shen L, Zhang B, Nestler
688 EJ. Circuit-wide Transcriptional Profiling Reveals Brain Region-Specific Gene Networks
689 Regulating Depression Susceptibility. Neuron. 2016 Jun 1;90(5):969-83.
690 https://10.1016/j.neuron.2016.04.015.
691 55. Wilkinson MB, Xiao G, Kumar A, LaPlant Q, Renthal W, Sikder D, Kodadek TJ, Nestler EJ.
692 Imipramine treatment and resiliency exhibit similar chromatin regulation in the mouse
693 nucleus accumbens in depression models. J Neurosci. 2009 Jun 17;29(24):7820-32.
694 https://10.1523/JNEUROSCI.0932-09.2009.

695

696 ***Author contribution***

697 Conceptualization, MEF, MKL, GK; Methodology, MEF, MKL, SA, GK; Formal analysis, GK,
698 MB; Investigation, MEF, DF, JO; Resources, MKL; Writing – Original Draft, GK, RC, MKL;
699 Reviewing & Editing, MKL, RC, MEF, SAA; Visualization, GK; Funding Acquisition, MEF, MKL

700

701 ***Funding***

702 This study was funded by NIH R01MH106500 to MKL. We would like to thank Maryland
703 Genomics within the UMSOM Institute for Genome Sciences for their RNA-sequencing
704 service.

705

706 ***Declaration of interests***

707 The authors of the paper have no financial or personal potential conflicts of interest

708

709 ***Figure legends***

710 Fig 1. A) Schematic of experimental design. D1-Cre-RT and A2A-Cre-RT female mice were
711 made to undergo the witness defeat paradigm for 10 days (10 minutes/day). 24 hours
712 following the last defeat, the mice went through the 3 Chamber Social Interaction Test
713 (3ChSI) after which they were sacrificed 24h later. The average time control mice spent in the
714 social chamber (D1- and A2A-Cre-RT controls combined) was used to classify mice has high

social interactors (higher than control average) or low social interactors (lower than control average). B) (left) Heatmap displaying localization of low social interactors (SI), high SI and control mice during the 3ChSI test. Areas highlighted in purple correspond with locations mice spend more time in while areas in yellow correspond with areas mice spent less time in. (right) Boxplots showing the time mice from each group spent in the interaction chamber (for each MSN subtype; one-way ANOVA: D1: $p\text{-value} < 0.05$, $F(2,57) = 45.09$; A2A: $p\text{-value} < 0.05$, $F(2,58) = 25.12$). The red dotted line represents the control group average, which was used to classify mice as low or high SI. C) (left to right) Venn diagrams visualizing the overlapping DEGs across stress groups in (top) D1- and (bottom) A2A-Cre-RT mice, bar plots of top differentially expressed genes (DEGs) between the stress groups in (top) D1- and (bottom) A2A-Cre-RT mice. D) Enrichment results for D1-MSN DEGs with the genes and terms color coded based on the DEG list they represent. E) Enrichment results for A2A-MSN DEGs with the genes and terms color coded based on the DEG list they represent.

Fig 2. A) Dendrogram of genes from the female D1-Cre-RT data with WGCNA module assignment represented in the colored bar below. B) Circos plots of the significant D1-MSN modules with each 'slice' corresponding with one module. The plot is organized based on the module eigengene dendrogram, shown in the center, which positions related modules close to one another. Modules that aren't significant are uncolored. C) Circular bar plots of D1-MSN modules significantly associated with high or low social interaction in female socially stressed mice. The proportion of the module that includes differentially expressed genes from the D1 high SI vs low SI comparison is highlighted in purple. D) Sankey plots of significantly differentially regulated modules in the D1-MSN of female socially stressed mice; modules are renamed based on their original WGCNA module number and functional categorization based on hub gene and enrichment analysis characterization.

Fig 3. A) Dendrogram of genes from the female A2A-Cre-RT data with WGCNA module assignment represented in the colored bar below. B) Circos plots of the significant A2A-MSN modules with each 'slice' corresponding with one module. The plot is organized based on the module eigengene dendrogram, shown in the center, which positions related modules close to one another. Modules that aren't significant are uncolored. C) Circular bar plots of A2A-MSN modules significantly associated with stress susceptibility and/or resilience in female socially stressed mice. The proportion of the module that includes differentially expressed genes from the A2A high SI vs low SI comparison is highlighted in purple. D) Sankey plots of significantly differentially regulated modules in the A2A-MSN of female socially stressed mice; modules are renamed based on their original WGCNA module number and functional categorization based on hub gene and enrichment analysis characterization.

751 Fig 4. Subtype-specific modules with the largest proportion of differentially regulated genes
752 between stress group selected for further analysis. A) (left, above) boxplot visualizing
753 expression level of F D1 M12 by stress group (left, below) bar chart visualizing the proportion
754 of genes in the D1 M12 module that are differentially regulated between the stress groups
755 (right, above) top hub genes from D1 M12 with change indicated to the right (right, below)
756 enrichment results for genes differentially expressed within the module. B) (left, above) box
757 plot visualizing expression level of F A2A M10 by stress group (left, below) bar chart
758 visualizing the proportion of genes in the D2 M10 module that are differentially regulated
759 between the stress groups (right, above) top hub genes from A2A M10 with change indicated
760 to the right (right, below) enrichment results for differentially expressed module genes. C)
761 Gene-concept network plot visualizing D1 M12 and D2 M10 genes involved in the PI3K-Akt
762 signaling pathway. D) (top) top transcription regulators identified using top genes from D1
763 M12 and (bottom) A2A M10. E) Enriched terms associated with NF1-regulated modular
764 genes.

765 Fig 5. A) cross-species consensus module analysis was performed using transcriptomic
766 data from male and female MDD NAc, D1- and D2-Cre-RT male mice that had undergone the
767 chronic social defeat stress paradigm (CSDS) and the female CWDS dataset. B) Dendrogram
768 of consensus module analysis with module assignment represented by the colored bars
769 below. C) Top hub genes from consensus module three Network plot visualizing the
770 consesus module 3. D) Boxplot of module 3 expression in (top) NAc of male and female
771 human, (middle) D1-MSN of stressed male and female mice and (bottom) A2A-MSN of
772 stressed male and female mice E) Enrichment analysis results of positive and negative
773 consensus module 3-scored genes.

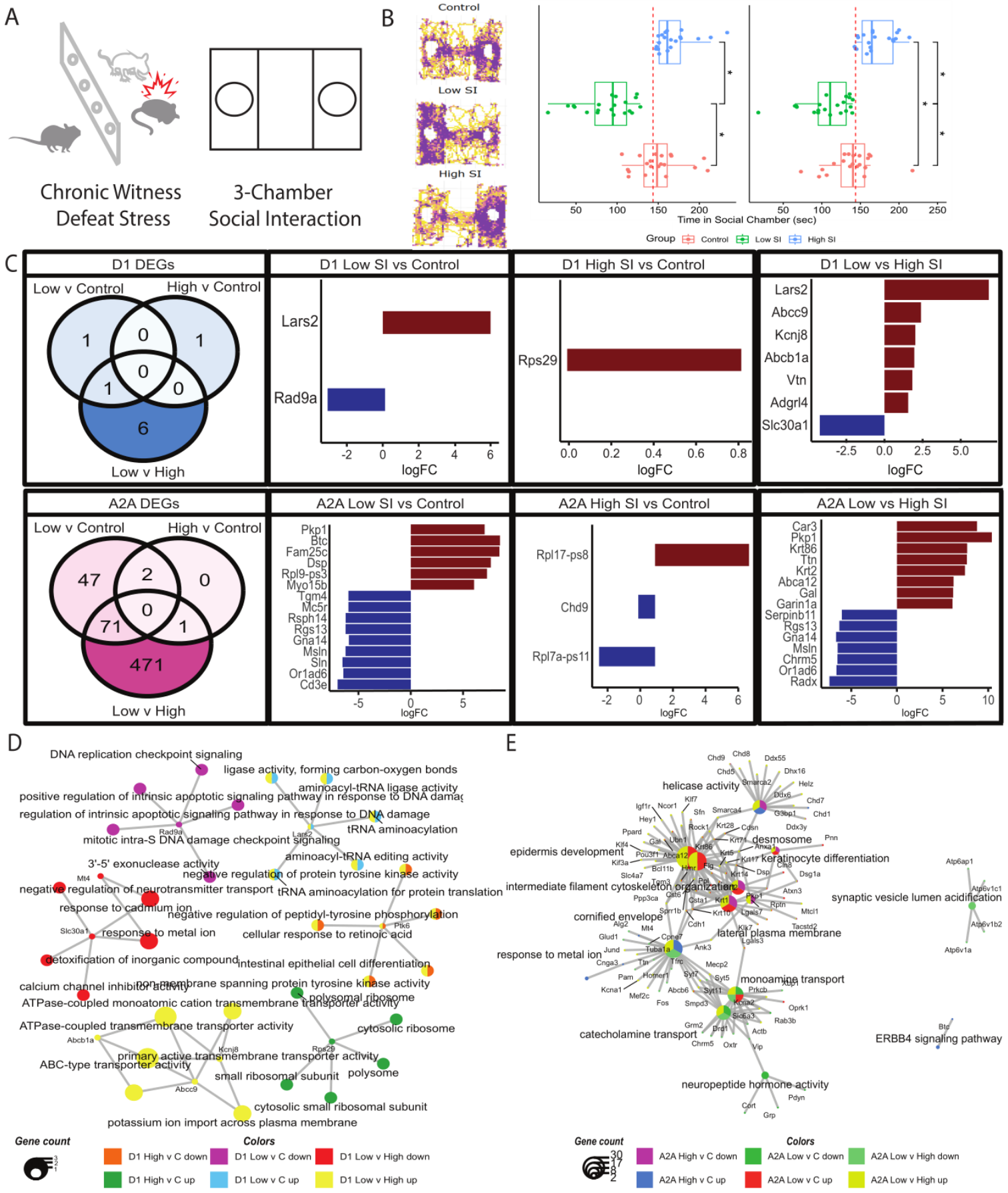

Fig 1. A) Schematic of experimental design. D1-Cre-RT and A2A-Cre-RT female mice were made to undergo the witness defeat paradigm for 10 days (10 minutes/day). 24 hours following the last defeat, the mice went through the 3 Chamber Social Interaction Test (3ChSI) after which they were sacrificed 24h later. The average time control mice spent in the social chamber (D1- and A2A-Cre-RT controls combined) was used to classify mice has high social interactors (higher than control average) or low social interactors (lower than control average) B) (left) Heatmap displaying localization of low social interactors (SI), high SI and control mice during the 3ChSI test. Areas highlighted in purple correspond with locations mice spend more time in while areas in yellow correspond with areas mice spent less time in. (right) Boxplots showing the time mice from each group spent in the interaction chamber (for each MSN subtype; one-way ANOVA: D1: p-value < 0.05, F(2,57) = 45.09; A2A: p-value < 0.05, F(2,58) = 25.12). The red dotted line represents the control group average. C) (left to right) Venn diagrams visualizing the overlapping DEGs across stress groups in (top) D1- and (bottom) A2A-Cre-RT mice, bar plots of top differentially expressed genes (DEGs) between the stress groups in (top) D1- and (bottom) A2A-Cre-RT mice. D) Enrichment results for D1-MSN DEGs with the genes and terms color coded based on the DEG list they represent. E) Enrichment results for A2A-MSN DEGs with the genes and terms color coded based on the DEG list they represent.

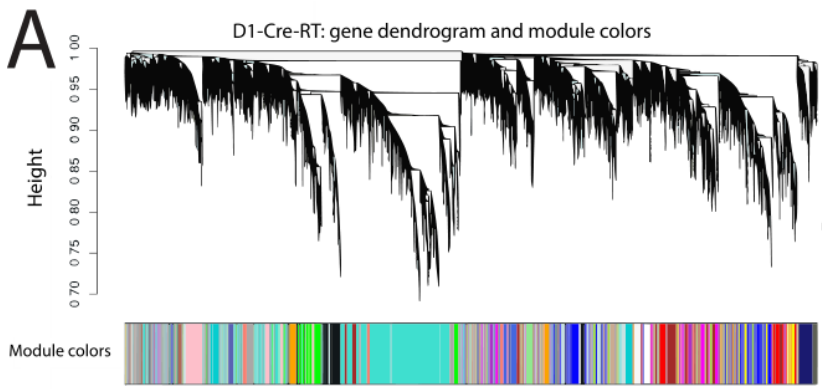
A
D1-Cre-RT: gene dendrogram and module colors
Height
Module colors

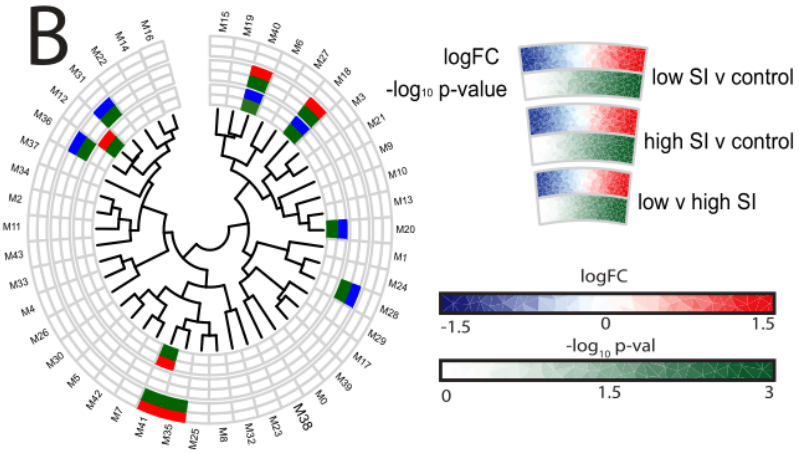
B
logFC
-log10 p-value
low SI v control
high SI v control
low v high SI
logFC
-1.5
0
1.5
-log10 p-val
0
1.5
3

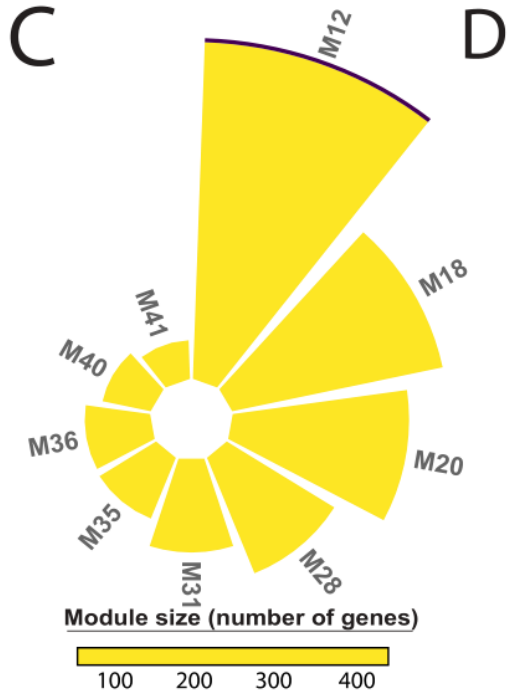
C
M12
M18
M20
M28
M31
M35
M36
M40
M41
Module size (number of genes)
100
200
300
400

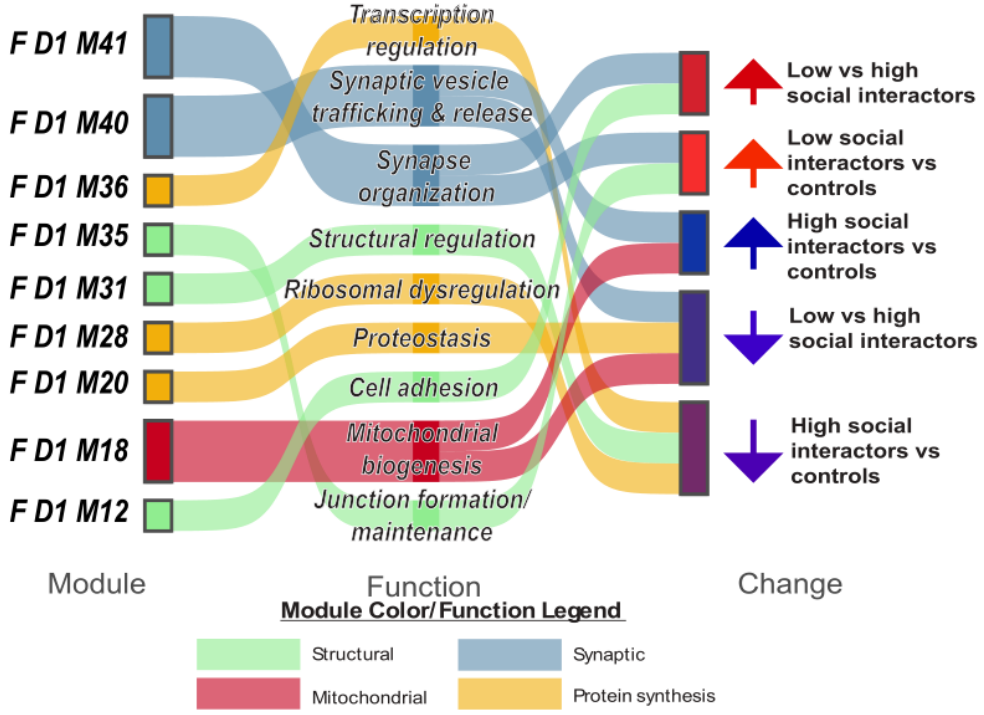
D
F D1 M41
F D1 M40
F D1 M36
F D1 M35
F D1 M31
F D1 M28
F D1 M20
F D1 M18
F D1 M12
Transcription regulation
Synaptic vesicle trafficking & release
Synapse organization
Structural regulation
Ribosomal dysregulation
Proteostasis
Cell adhesion
Mitochondrial biogenesis
Junction formation/ maintenance
Low vs high social interactors
Low social interactors vs controls
High social interactors vs controls
Low vs high social interactors
High social interactors vs controls
Module
Function
Change
Module Color/ Function Legend
Structural
Synaptic
Mitochondrial
Protein synthesis

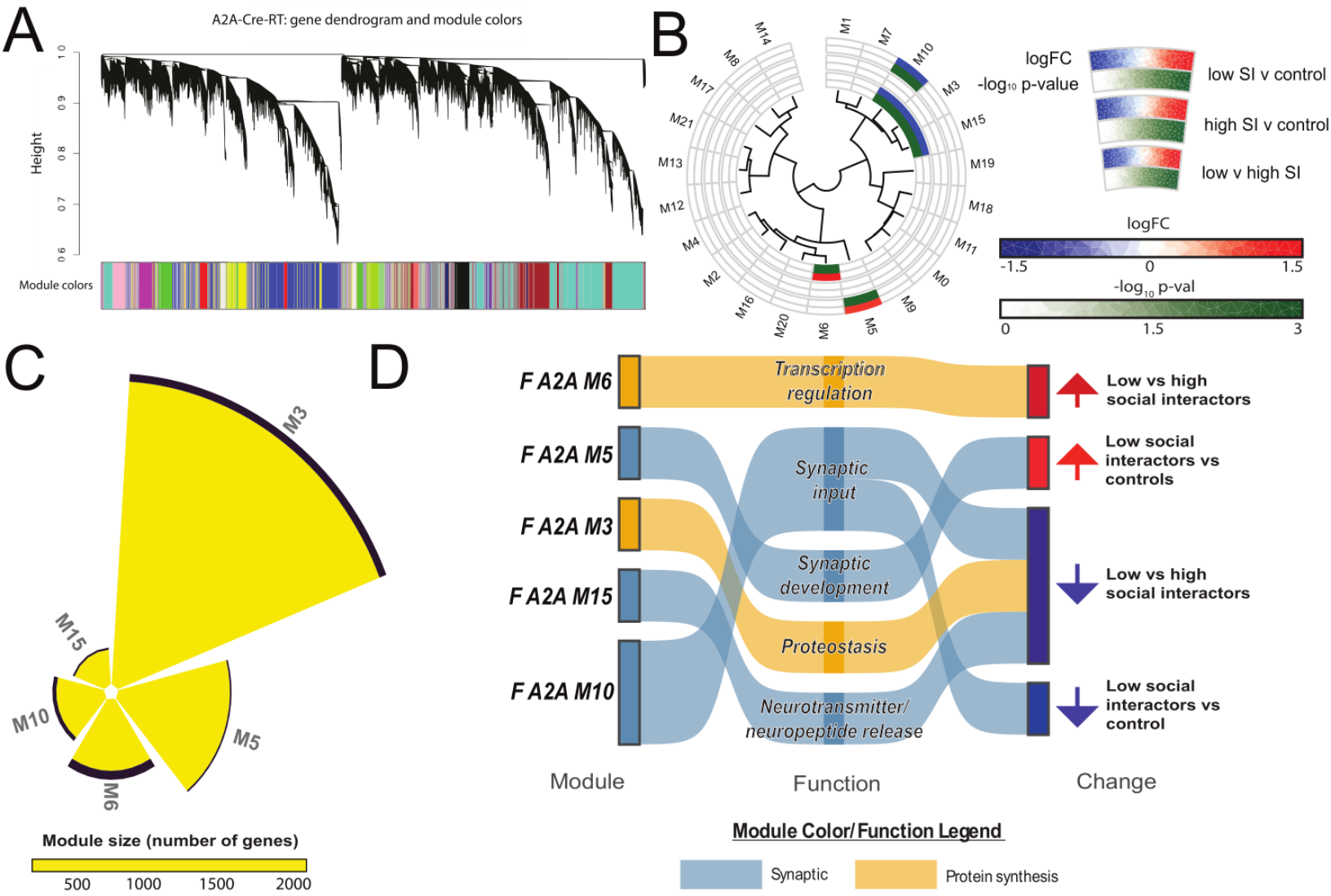
A
A2A-Cre-RT: gene dendrogram and module colors
Height
Module colors
B
M1
M7
M10
M3
M15
M19
M18
M11
M0
M9
M5
M6
M20
M16
M2
M4
M12
M13
M21
M17
M8
M14
logFC
-log10 p-value
low SI v control
high SI v control
low v high SI
logFC
-1.5
0
1.5
-log10 p-val
0
1.5
3
C
M3
M15
M10
M5
M6
Module size (number of genes)
500
1000
1500
2000
D
F A2A M6
F A2A M5
F A2A M3
F A2A M15
F A2A M10
Transcription regulation
Synaptic input
Synaptic development
Proteostasis
Neurotransmitter/ neuropeptide release
Low vs high social interactors
Low social interactors vs controls
Low vs high social interactors
Low social interactors vs control
Module
Function
Change
Module Color/ Function Legend
Synaptic
Protein synthesis

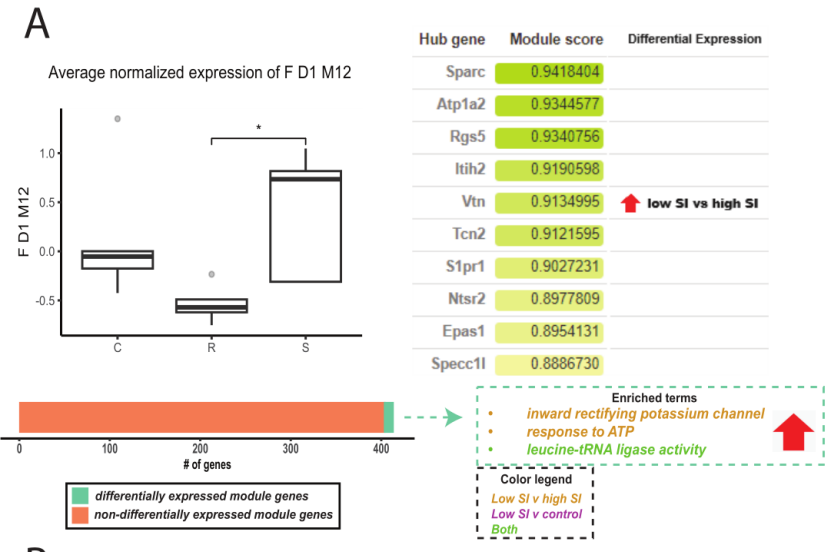
A
Average normalized expression of F D1 M12
F D1 M12
C
R
S
# of genes
differentially expressed module genes
non-differentially expressed module genes
Hub gene
Module score
Differential Expression
Sparc 0.9418404
Atp1a2 0.9344577
Rgs5 0.9340756
Itih2 0.9190598
Vtn 0.9134995
low SI vs high SI
Tcn2 0.9121595
S1pr1 0.9027231
Ntsr2 0.8977809
Epas1 0.8954131
Specc1l 0.8886730
Enriched terms
inward rectifying potassium channel
response to ATP
leucine-tRNA ligase activity
Color legend
Low SI v high SI
Low SI v control
Both

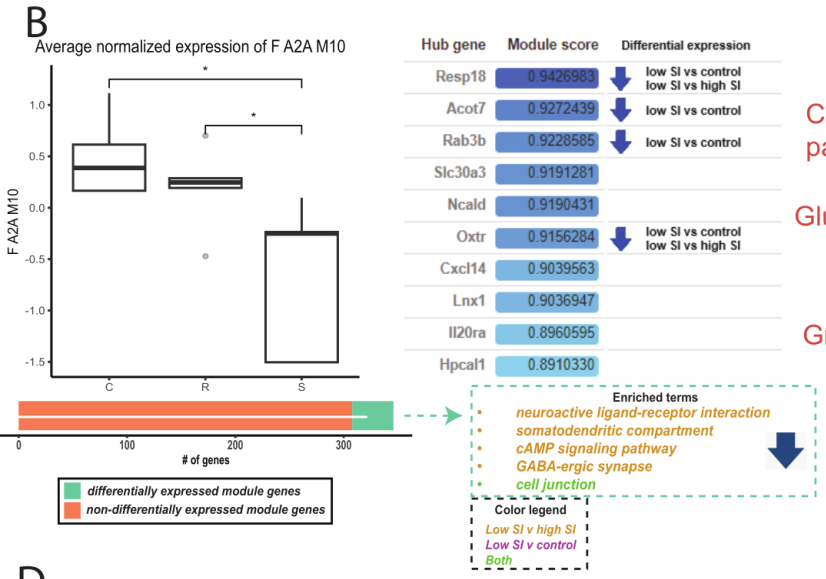
B
Average normalized expression of F A2A M10
F A2A M10
C
R
S
# of genes
differentially expressed module genes
non-differentially expressed module genes
Hub gene
Module score
Differential expression
Resp18 0.9426983
low SI vs control
low SI vs high SI
Acot7 0.9272439
low SI vs control
Rab3b 0.9228585
low SI vs control
Slc30a3 0.9191281
Ncald 0.9190431
Oxtr 0.9156284
low SI vs control
low SI vs high SI
Cxcl14 0.9039563
Lnx1 0.9036947
Il20ra 0.8960595
Hpcal1 0.8910330
Enriched terms
neuroactive ligand-receptor interaction
somatodendritic compartment
cAMP signaling pathway
GABA-ergic synapse
cell junction
Color legend
Low SI v high SI
Low SI v control
Both

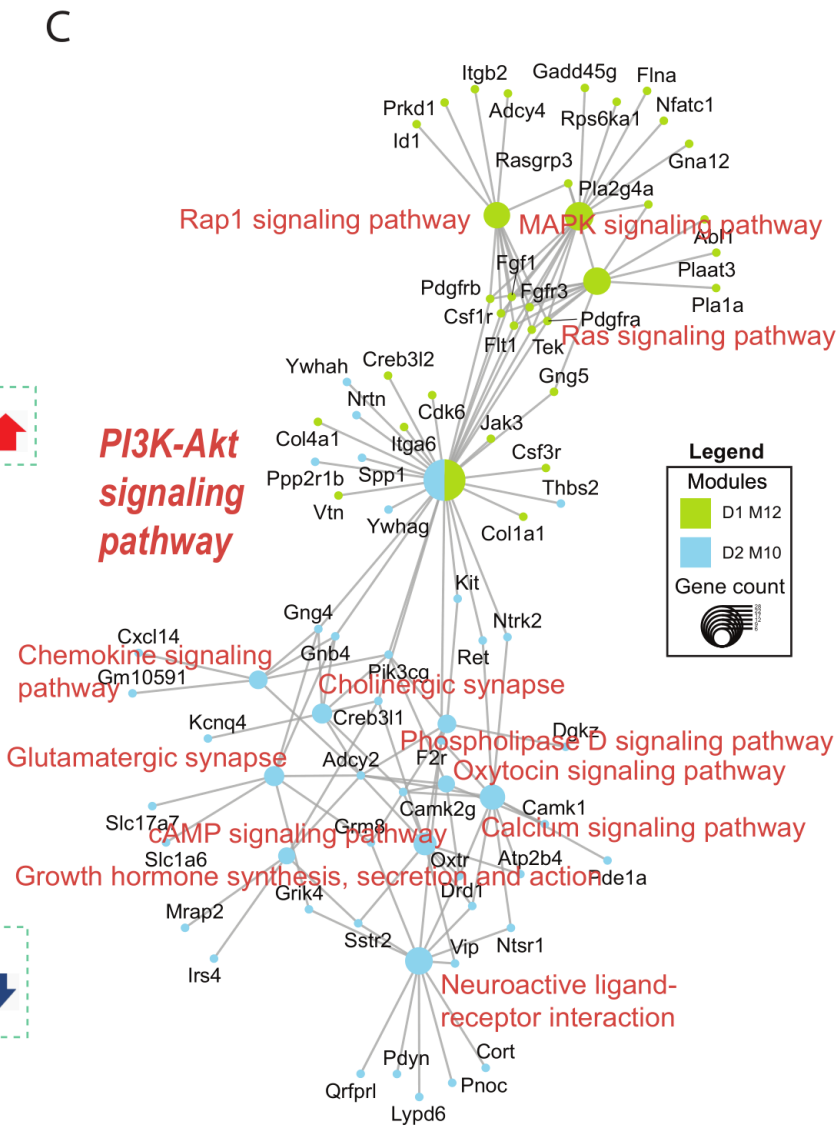
C
Rap1 signaling pathway
MAPK signaling pathway
Ras signaling pathway
PI3K-Akt signaling pathway
Chemokine signaling pathway
Cholinergic synapse
Glutamatergic synapse
Phospholipase D signaling pathway
Oxytocin signaling pathway
cAMP signaling pathway
Calcium signaling pathway
Growth hormone synthesis, secretion and action
Neuroactive ligand-receptor interaction
Itgb2
Gadd45g
Flna
Prkd1
Adcy4
Rps6ka1
Nfatc1
Id1
Rasgrp3
Gna12
Pla2g4a
Abl1
Fgf1
Plaat3
Pdgfrb
Fgfr3
Pla1a
Csf1r
Pdgfra
Flt1
Tek
Ywhah
Creb3l2
Gng5
Nrtn
Cdk6
Jak3
Col4a1
Itga6
Csf3r
Ppp2r1b
Spp1
Thbs2
Vtn
Ywhag
Col1a1
Kit
Gng4
Ntrk2
Cxcl14
Gnb4
Ret
Gm10591
Pik3cg
Kcnq4
Creb3l1
Dgkz
Adcy2
F2r
Slc17a7
Camk2g
Camk1
Grm8
Slc1a6
Oxtr
Atp2b4
Pde1a
Grik4
Drd1
Mrap2
Sstr2
Vip
Ntsr1
Irs4
Pdyn
Cort
Qrfprl
Pnoc
Lypd6
Legend
Modules
D1 M12
D2 M10
Gene count

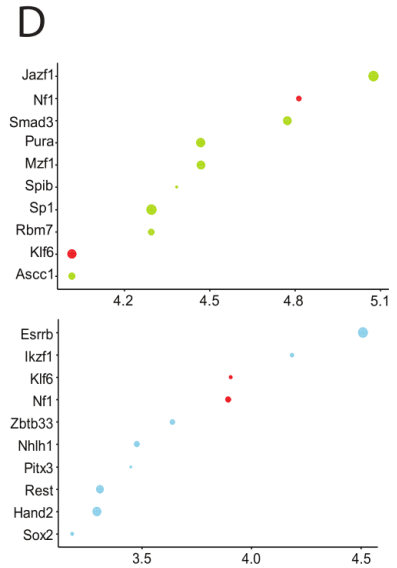
D
Jazf1
Nf1
Smad3
Pura
Mzf1
Spib
Sp1
Rbm7
Klf6
Ascc1
4.2
4.5
4.8
5.1
Esrrb
Ikzf1
Klf6
Nf1
Zbtb33
Nhlh1
Pitx3
Rest
Hand2
Sox2
3.5
4.0
4.5

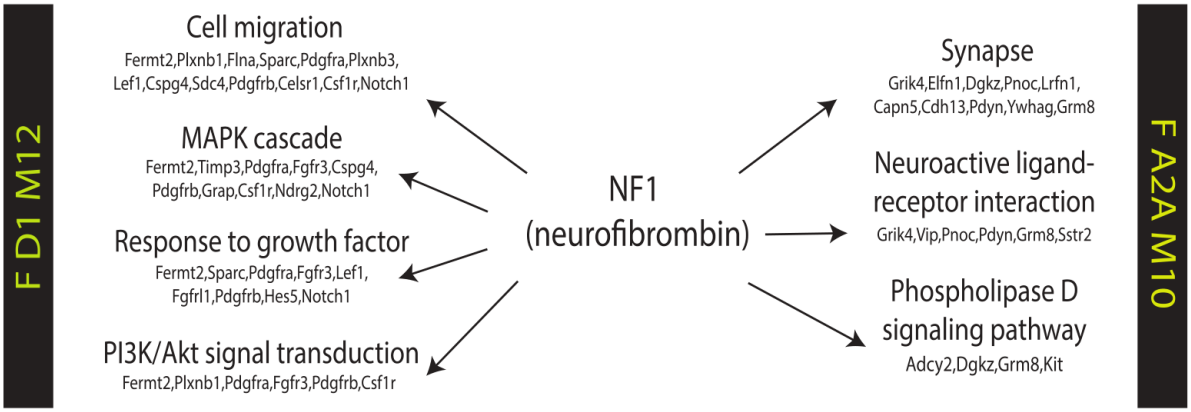
E
F D1 M12
Cell migration
Fermt2,Plxnb1,Flna,Sparc,Pdgfra,Plxnb3,
Lef1,Cspg4,Sdc4,Pdgfrb,Celsr1,Csf1r,Notch1
MAPK cascade
Fermt2,Timp3,Pdgfra,Fgfr3,Cspg4,
Pdgfrb,Grap,Csf1r,Ndrg2,Notch1
Response to growth factor
Fermt2,Sparc,Pdgfra,Fgfr3,Lef1,
Fgfrl1,Pdgfrb,Hes5,Notch1
PI3K/Akt signal transduction
Fermt2,Plxnb1,Pdgfra,Fgfr3,Pdgfrb,Csf1r
NF1
(neurofibrombin)
Synapse
Grik4,Elfn1,Dgkz,Pnoc,Lrfn1,
Capn5,Cdh13,Pdyn,Ywhag,Grm8
Neuroactive ligand-
receptor interaction
Grik4,Vip,Pnoc,Pdyn,Grm8,Sstr2
Phospholipase D
signaling pathway
Adcy2,Dgkz,Grm8,Kit
F A2A M10

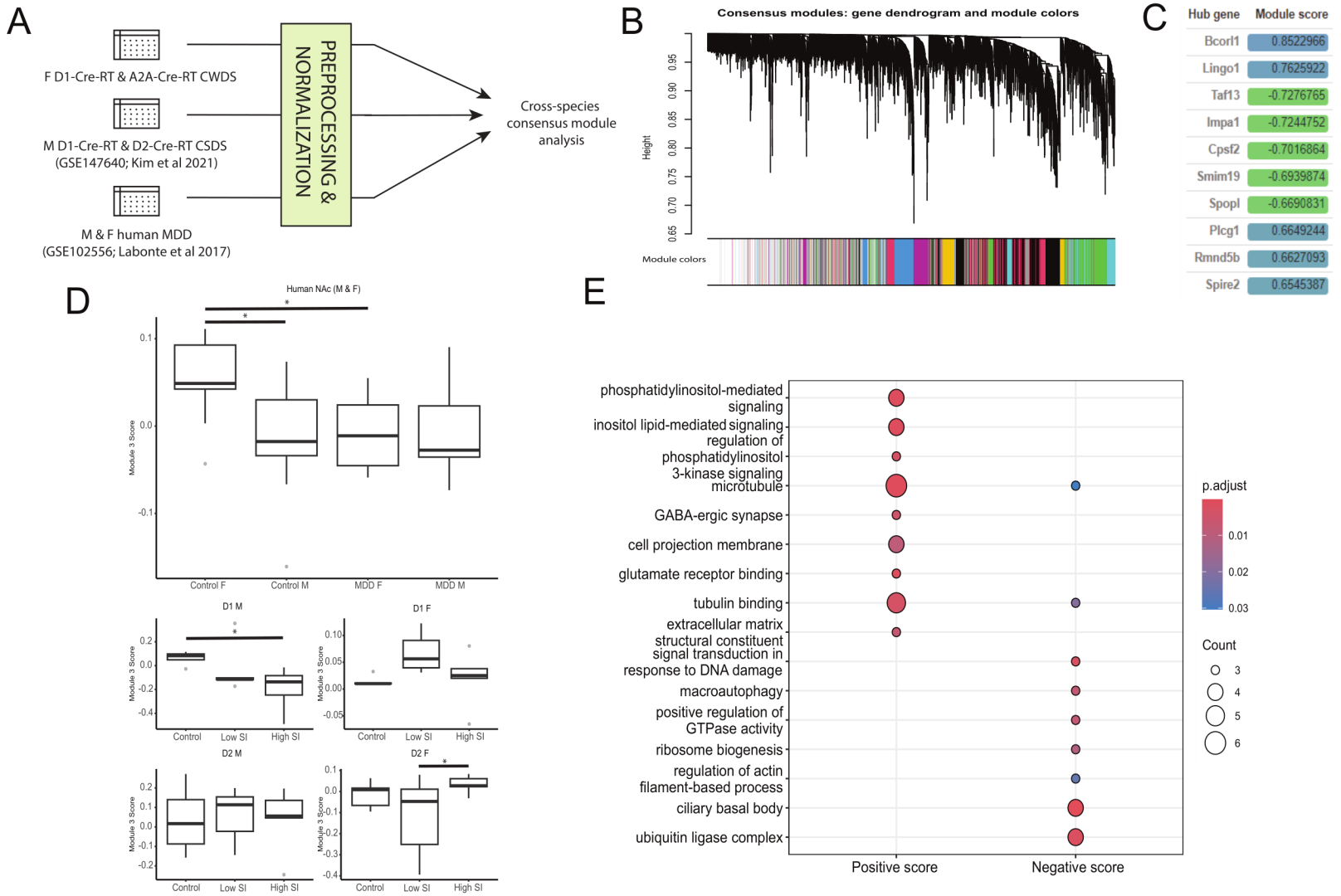
A
F D1-Cre-RT & A2A-Cre-RT CWDS
M D1-Cre-RT & D2-Cre-RT CSDS
(GSE147640; Kim et al 2021)
M & F human MDD
(GSE102556; Labonte et al 2017)
PREPROCESSING & NORMALIZATION
Cross-species consensus module analysis
B
Consensus modules: gene dendrogram and module colors
Height
Module colors
C
Hub gene
Module score
Bcorl1 0.8522966
Lingo1 0.7625922
Taf13 -0.7276765
Impa1 -0.7244752
Cpsf2 -0.7016864
Smim19 -0.6939874
Spopl -0.6690831
Plcg1 0.6649244
Rmnd5b 0.6627093
Spire2 0.6545387
D
Human NAc (M & F)
Module 3 Score
Control F
Control M
MDD F
MDD M
D1 M
D1 F
D2 M
D2 F
Control
Low SI
High SI
E
phosphatidylinositol-mediated signaling
inositol lipid-mediated signaling
regulation of phosphatidylinositol 3-kinase signaling
microtubule
GABA-ergic synapse
cell projection membrane
glutamate receptor binding
tubulin binding
extracellular matrix
structural constituent
signal transduction in response to DNA damage
macroautophagy
positive regulation of GTPase activity
ribosome biogenesis
regulation of actin filament-based process
ciliary basal body
ubiquitin ligase complex
Positive score
Negative score
p.adjust
0.01
0.02
0.03
Count
3
4
5
6